ejpmr, 2021,8(5), 655-664

SJIF Impact Factor 6.222

EUROPEAN JOURNAL OF PHARMACEUTICAL AND MEDICAL RESEARCH

www.ejpmr.com

Research Article

ISSN 2394-3211

EJPMR

ALUMINIUM CHLORIDE PHTHALOCYANINE VIA HEXAGONAL LIQUID CRYSTAL NANODISPERSION EFFICIENTLY INHIBITS TUMOUR CELL GROWTH AND INDUCES NUCLEUS DAMAGE AFTER PHOTODYNAMIC THERAPY

Tulio Ruiz Eschiapati[1], Jessica Bidurin Picolo[1], Bruna Stangherlin[1], Gustavo Gonçalves Maciel[1], Fabiola Garcia Praça[2], Juliana Rosa Viegas[2], Ana Vitoria Silvestrini[2], José Orestes Del Ciampo[2], Maria Vitoria Lopes Badra Bentley[2] and Wanessa Silva Garcia Medina[1]*

[1]University Center Padre Albino, UNIFIPA- Catanduva- São Paulo, 15809-144, Brazil.
[2]School of Pharmaceutical Sciences of Ribeirão Preto – University of São Paulo, Ribeirão Preto, São Paulo, 14040-903, Brazil.

***Corresponding Author: Dr. Wanessa Silva Garcia Medina**

University Center Padre Albino, UNIFIPA- Catanduva- São Paulo, 15809-144, Brazil.

Article Received on 17/03/2021 **Article Revised on 07/04/2021** **Article Accepted on 28/04/2021**

ABSTRACT

Topical photodynamic therapy (PDT) is a two-stage therapy which combines the use of photosensitizing drugs and light energy activating a cascade of phototoxic reactions and consequent tumor death. PDT has been applied to almost every type of cancers including melanoma. Aluminum chloride phthalocyanine (AlClPc) is a lipophilic photosensitizer widely used in preclinical studies of PDT for the treatment of skin cancer.[5] Besides AlClPc has excellent photochemical and photodynamic activity, this is insoluble in water, which limits its bioavailability and its administration in a physiological environment. In this scenario, several strategies have been proposed to improve the skin accumulation of photosensitizers, mainly the use of drug delivery system-based nanotechnology. In this study, we described the preparation and characterization of hexagonal liquid crystalline nanodispersion (LCN) as drug delivery system-based nanotechnology for AlClPc. Also, in vitro phototoxicity effect on A375 cells and cell damage, were evaluated to investigate its efficacy in PDT. AlClPc-loaded LCN was characterized according to their particle size, distribution and zeta potential, morphological aspects by atomic force microscopy, stability and phototoxic action in melanoma cell line (A375). The means of particle size were 198.56 (±1.0) and 179.7 (±2.0) for LCN in absence or AlClPc presence, respectively. Negative zeta potential was approximately 40 and AlClPc-loaded LCN maintained their physical stability from particle size and distribution over 15 days. In addition, AlClPc-loaded LCN also presented biocompatibility in the dark for normal keratinocytes cell (HaCat) from 4 to 1300ng/mL and potent antitumor effect in PDT using 1J/cm^2 for melanoma cell (A375) with nuclear cell damage at 300ng/mL. This study demonstrated that AlClPc-loaded LCN is a potent and promising drug delivery system-based nanotechnology for use in PDT.

KEYWORD: Photodynamic Therapy, Liquid crystal nanodispersion, Chloro-aluminium phthalocyanine, tumor cells, cancer treatment.

1. INTRODUCTION

Photodynamic therapy (PDT) comprises an alternative and promising therapeutic line for controlling, treatment and diagnosis of malignant diseases. PDT treatment is based on administration of photosensitizer drugs (PS) and its selective retention in malignant tissue which, after light activation at specific wavelengths, excites and triggers photochemical reactions that generate free radicals and / or reactive species of oxygen (ROS) causing local cell destruction (Medina et al., 2011).

This therapy has been studied and used as an experimental modality in numerous countries for the treatment of several types of tumors, including melanoma skin cancer (MSC), (Koechli, et al., 2015). The MSC has its origin in the melanin-producing cells, the melanocytes. During this pathological procedure, a series of cell mutations can occur, mainly in the epidermis layer, promoting the invagination and metastasis of tumor cells (Borgheti-Cardoso, et al., 2020; Krattinger et al., 2018). However, the challenge of PDT applied to skin cancer is to reach accumulation of photosensitizers into the melanoma cells after its topical application. This is because most PS has hydrophobic character which makes it difficult to optimal formulation prepare as well as its dermal penetration. Thus, several studies are currently being conducted focusing on increasing the PS skin penetration based on nanotechnology.

Substances such as phthalocyanines represent a pioneering role in the modernization of drugs for therapeutic strategy in PDT, since they have an advantage in selective retention in tumor cells, ease of synthesis, resistance to chemical and photochemical degradation, intensification of the production of reactive oxygen species and low toxicity in the absence of luminosity (Zhia et al., 2020).

Chloro-aluminum phthalocyanine (ClAlPc), in turn, is a lipophilic PS used in preclinical PDT studies for the specific treatment of skin cancer. ClAlPc contain aluminum as a central metal ion (**Figure 1**), in which increases photophysical and photo-chemical properties of this PS. Also, ClAlPc presents molar absorption coefficient around 600 nm, favoring the use of red laser capable of penetrating to the basal layer of the skin, where the tumor is and activating the skin accumulated PS (Lucky et al., 2015).

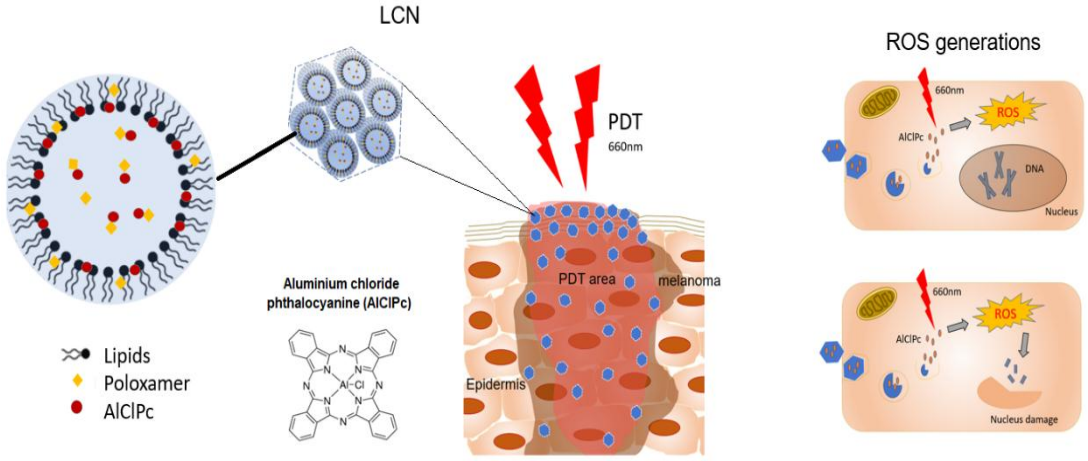

Figure 1. Structural hexagonal liquid crystalline nanoparticles, molecular Aluminium chloride phthalocyanine, PDT application on skin cancer and ROS generation.

On the other hand, due to the highly hydrophobic character of AlClPc, it cannot be easily solubilized in the solvents commonly used to topical administration, in addition, it can present aggregation in the aqueous environment causing molecule degradations that reduces its photodynamic efficacy (Rossetti et al., 2011). To overcome this limitation, delivery systems based on nanotechnology is required. In this context, we chose to evaluate the effectiveness of liquid crystalline system as a drug delivery system for AlClPc in PDT.

Liquid crystalline systems based on lipid and aqueous phase can form both lamellar and cubic phases while hexagonal phases required the use of additive as oleic acid. In general, cubic and hexagonal phases after its dispersion in excess of aqueous phase, are extremely stable nanoparticles capable of protecting bioactive compounds against photodegradation (Ferreira, et al., 2009) and, consequently, they are widely recognized for presenting greater efficiency in this directed dermal delivery (Praça et al., 2020).

Hexagonal phase can be obtained in a normal or reverse structure depending on the preparation process and components used (review Ana). When hexagonal phase is obtained in the presence of oleic acid, as obtained in this work, it forms in a reverse position displaying large quantity of densely packed water filled cylindrical micelles, following a long-range order two-dimensional lattice (Huang et al., 2018) with a negative mean curvature towards the aqueous interior.

In this study, we demonstrated that hexagonal liquid crystalline nanodispersion (LCN) can be a promising drug delivery system-based on nanotechnology for AlClPc used in PDT. From that, an in vitro laboratory test with tumoral A375 cells was performed in order to evaluate its phototoxicity effect and investigate its applicability in PDT for melanoma-like skin cancer.

2. MATERIALS AND METHODS

2.1 Preparation of hexagonal liquid crystalline phase nanodispersion

The hexagonal liquid crystalline gel phase was prepared by mixing monoolein which was first melted at 42ºC followed by the addition of oleic acid and citrate buffer solution (pH 6.0) containing 1.5% of poloxamer 407 to produce a monoolein/oleic acid/ citrate buffer system (7.7:0.5:81.8, w/w/w). The AlClPc, pre-dissolved in DMSO, was added to the lipid phase (monoolein/oleic acid mixture) to produce a monoolein/oleic acid/AlClPc/citrate buffer system (7.7:0.5:0.03:81.76, w/w/w, w/w/w/w/w). The system was allowed to equilibrate at room temperature for 24 h. After hexagonal liquid crystalline phase was confirmed by polarized light microscopy the formulation was vortex-mixed and sonicated in an ice bath for 1 min to produce the liquid crystalline nanodispersion system (LCN).

2.2 Physicochemical characterization

2.2.1 Polarized light microscopy

The hexagonal liquid crystalline gel phase was characterized from fanlike and angular texture standard under a polarized light microscope (Axioplan 2 Image Pol microscope, Carl Zeiss, Oberkochen, Germany) within 24 hours after preparation.

2.2.2 Dynamic Light Scattering (DLS) and Nanoparticle Tracking Analysis (NTA)

The mean particle size, particles dispersion, surface charge as well as nanoparticle tracking of the CLN were evaluated by DLS and NTA respectively. The CLN was diluted (1:400, v/v) in particle-free ultra-purified water or KCL solution (0.1M) for particle size or zeta potential respectively and the measurements were performed using a Zetasizer Nano ZS instrument (Malvern Instruments, Worcestershire, United Kingdom) equipped with a 633-nm He-Ne laser operating at an angle of 173°. The zeta potential was determined by electrophoretic mobility of dispersed particles under an electrical field, using the same instrument.

NTA was performed with a NanoSight NS300 (Malvern, United Kingdom) equipment with NTA 3.1 Build 3.1.54 software in a coupled chamber with a 642 nm laser (output power 40 mW). The LCN were diluted (1:5000, v/v) in particle-free ultra-purified water and injected into the sample chamber with a sterile syringe (BD Plastipak, Parana, Brazil) until the liquid reached the tip of the nozzle. The data represent the average values from three separate measurements. The result was expressed by average particle size ± standard deviation values obtained with NTA software.

2.2.3 Physical stability

The physical stability of the AlClPc -loaded LCN system (n=3) was determined over a period of 15 days at room temperature (25 ºC, approximately). The humidity was unaccounted for. The physical stability of the formulations with respect to the mean diameter and polydispersity index (Pld) were evaluated by DLS. The data represented the mean values and standard deviation from three separate measurements.

2.2.4 Atomic force microscopy (AFM)

The morphological analysis of the nanoparticle by AFM was performed using a Shimadzu SPM-9600 scanning microscope. For this, the samples were diluted (1: 400, v / v) in particle-free ultra-purified water and then, droplet of the LCN were deposited on a freshly cleaved mica surface and dried under argon flow. The measurements were performed using a silicon cantilever and resonance frequency of 300 kHz and an elastic constant of 40 N / m.

2.3 In vitro biocompatibility test and dark cytotoxicity

The A375 (melanoma) and HaCaT (human keratinocytes) cells line were cultured in 75 cm^2 flasks with high glucose DMEM, 10% FBS and antibiotics (100 IU/mL of penicillin and streptomycin, as well as 250 ng/mL of amphotericin-B) at 37 ºC with 5% CO_2. Before applying the PDT the cell viability of unloaded CLN and AlClPc -loaded LCN on normal and cancerous cells was investigated under dark conditions. In 96-well plates, 10^4 cells were placed per well, approximately 24 hours prior to the cell viability assay. Then, culture medium was removed and replaced with medium containing various volumes of unloaded LCN and AlClPc -loaded LCN at final concentration in the range of 4 to 1300 ng/mL. The viable and death cells which were cells untreated and cells treated with 30% Dimethyl sulfoxide respectively, were performed as controls.

After 24 hours, the cells were washed with PBS and incubated with a mixture of DMEM and resazurin dye (0.025mg/mL) for 4 hours. The samples were measured at excitation of 530/25, emission of 590/35 and gain of 35 in a BioStack Ready (Biotec Synergy 2, USA). The relative cell viability (%) compared to control cells was calculated by [abs] sample/ [abs] control × 100.

2.4 Intracellular localization

The A375 cells line was used to cellular transfection assay and intracellular localization evaluation. For this, the cells were seeded on cover slips, in 12-well plate at a density of 5.10^5 cells/well and incubated in complete growth medium for 24 h to allow cell adherence. The AlClPc-loaded LCN previously diluted at final concentration of 30 ng/mL was applied on the cells and incubate for 24 hours. Then, the cells were washed with PBS and fixed with a 1% glutaraldehyde solution. The excess of glutaraldehyde was removed with PBS and a solution with DAPI (0.3 µg/mL) was applied to the cells for 10 minutes. The cells were washed 3 times with PBS, to remove the DAPI excess and the cover slips were transferred into a glass slide with a drop of Fluoromount™. Intercellular localization of AlClPc -loaded LCN was imaged using a confocal microscopy CLSM with a 63× immersion objective, λ = 405 nm and λ = 630 lasers, suitable for DAPI, and AlClPc, respectively.

2.5 Photodynamic therapy application

2.5.1 Laser chosen

Two different irradiation doses were performed on A375 incubation with AlClPc -loaded LCN (from 16 to 650 ng/mL) during 24 hours to select the PDT irradiation protocol. A Therapy EC laser equipment (DMC, U.S.A, Florida) was used and cells were exposed to red laser operating at energy density of 1 and 6 J/cm^2. All irradiations were accomplished under the following conditions: wavelength of 660 nm (± 10 nm) and power set to 100 mW. After irradiation, the cells were washed with PBS and incubated with a mixture of DMEM and resazurin dye (0.025mg/mL) for 4 hours. The samples were measured at excitation of 530/25, emission of 590/35 and gain of 35 in a BioStack Ready (Biotec Synergy 2, USA). The relative cell viability (%)

compared to control cells was calculated by [abs] sample/ [abs] control × 100.

2.5.2 Cell Treatment

The A375 cells were incubated for 24 hours as described in 2.3. Then, culture medium was removed and replaced with medium containing various volumes of AlClPc -loaded LCN at final concentration in the range of 4 to 300 ng/mL. After 1h of the treatment beginning, the cells were irradiated with red laser at 660 nm (± 10 nm), power set to 100mW and energy density of 1 J/cm^2 and the PDT efficacy was evaluated by resazurin dye (0.025mg/mL) for 4 hours. The samples were measured at excitation of 530/25, emission of 590/35 and gain of 35 in a BioStack Ready (Biotec Synergy 2, USA). The same protocol was applied in the dark (without PDT).

2.5.3 Cell Migration assay

Following treatment with AlClPc -loaded LCN (30 and 300 ng/mL) in a 12 well plate containing A375 cells (10^4 cells placed per well) for 24 h. After laser irradiation (at 1J/cm^2), in each well, was produced a scratch "mock wound" by gliding the sterile pipette tip across cell surface, producing a strip with very few cells at the bottom of the each well. Then, the cells were visualized and photographed under a microscope (10X magnitude), after 24 and 48 hours of the incubation.

2.5.4 Intracellular generation of reactive oxygen species (ROS)

After PDT in A 375 cells treated with AlClPc -loaded LCN (30 and 300 ng/mL) for 24 hours, the culture medium was replaced with a solution of 2′-7′-dichlorodihydrofluorescein diacetate (DCFDA) probe. Untreated cells were used as a control. After incubating for 4 h, cells were washed with PBS and identification of intracellular ROS using oxidized DCFDA was examined by fluorescence microscopy (Axioskop 2 plus, Carl Zeiss, Göttingen, Germany) using band-pass excitation and emission filters at 470/510 nm, suitable for 2′-7′-dichlorofluorescein (DCF), with a 20X objective.

2.5.5 Nucleus damage assay

Following treatment with AlClPc -loaded LCN diluted in culture medium to 30 and 300 ng/mL in A375 cells for 24 h, nuclear staining was performed with 0.3 μg/ml DAPI solution at 37˚C for 10 min. Untreated cells were used as control. A fluorescence microscopy (Axioskop 2 plus, Carl Zeiss, Göttingen, Germany) with band-pass excitation and emission filters at 450/490 nm (filter Set 50, Carl Zeiss) was used. Images were recorded with a light-sensitive charge-coupled device digital camera using identical sensitivity and exposure settings across all samples**.**

2.6 Statistical analysis

Data were presented as the average of three independent experiments ± standard errors and differences between groups were evaluated using one-way ANOVA followed by the Bonferroni post hoc test.

2. RESULTS AND DISCUSSION

In the present study, we developed a liquid crystalline dispersion system for skin delivery of AlClPc (AlClPc-LCN) based on monoolein and oleic acid which provided very satisfactory results for induce tumor cell damage after PDT.

In the last decade, different forms of LCN have shown promising results as delivery systems applied to delivery of drugs, bio-drugs and other actives (Silvestrini et al., 2020). In general, these LCN consisted of a phase mixture from lipid and aqueous phase in the presence or absence of additives (Silvestrini et al., 2020; Zhai et al., 2019; Manaia et al., 2017). Herein, we used a mixture phase of lipids (monoolein/oleic acid/AlClPc) and aqueous phase (citrate buffer solution containing 1.5% of poloxamer 407) giving rise to a bulk liquid crystalline gel.

Then, this gel was dispersed in excess of aqueous phase to form the nanoparticles (LCN), composed of monoolein/oleic acid/AlClPc/citrate buffer system (7.7:0.5:0.03:81.76, w/w/w, w/w/w/w/w). Fig. 1A illustrates the morphological aspects from AlClPc-loaded LCN by polarized and atomic force microscopy. The bulk liquid crystalline gel characteristic by polarized microscopy confirmed a well-defined hexagonal liquid crystalline structure with birefringence from the fan-like texture **(Figure 2. A)**. It is widely known that amphiphilic molecules, water content and addition of additives in liquid crystalline phases can lead to phase transition and consequently change the characteristics of the delivery system (Silvestrini et al., 2020; Huang et al., 2018; Fong et al., 2012). For this reason, we evaluated the influence of AlClPc into liquid crystalline gel by polarized microscopy (**Figure 2.B**) and we proved that addition of photosensitizer did not influence the phase transition of the liquid crystalline system which kept the hexagonal phase stable in the presence and absence of the drug.

Furthermore, the AFM images provided additional evidence for the hexagonal morphological aspect of the of the particles and its nanometer size **(Figure 2. C)**. The LCN did not displayed a spherical structure but rather a cylindrical structure with a long-range positional order of hexagonal lattice in two dimensions, with the length of these cylindrical superstructures reaching approximately 100 to 200 nm. Zhai and colleagues (2019) described that hexagonal phase consists of a group of micellar cylinders packed onto a 2-D hexagonal lattice (Zhai et al., 2019), when hexagonal phase is obtained in the presence of oleic acid, as obtained in this work, it forms in a reverse position displaying a negative mean curvature towards the aqueous interior. Over the past decade our research group has shown hexagonal phase by SAXS peaks in the ratio of 1: √3: √4. (Campos et al., 2020; Rossetti et al., 2016; Petrilli et al., 2016; Praça et al., 2012).

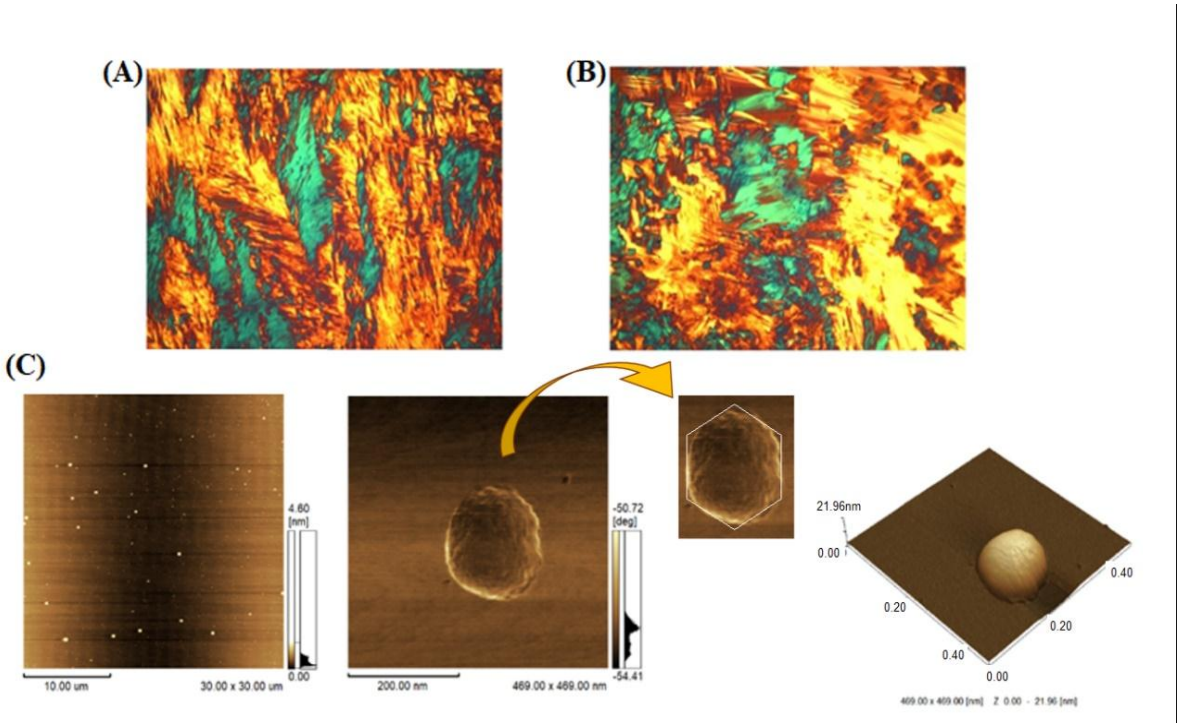

Figure 2. Characterization of the LCN in absence (A) and presence of AlClPc (B) by polarized microscopy, and morphological aspect under two and three-dimensional micrographs of the LCN obtained by atomic force microscopy (C).

The particle size, polydispersity index, zeta potential and values of particles/mL of both unloaded LCN and LCN containing AlClPc were determined by DLS and NTA (**Figure 3. A**). The results showed particle size less than 200 nm, narrow polydispersity index (≤ 0.28) and an average of $1.9x10^{12}$ particles/ mL dispersion, but when AlClPc was incorporated into the system, significant decreased in particle sizes from 198.5 (± 1.0) to 179.7 (± 2.0) nm ($p \leq 0.05$) was observed. Considering our research group expertise in developing liquid crystalline-based nanoparticles, we believe that the presence of hydrophilic AlClPc molecules into the LCN interferes on the interfacial water content, provoking a decrease in the water molecules accessible to hydrate the monoolein hydrophilic groups, producing more ordered and compacted structure (Campos et al., 2020). Also, significant increase was evidenced in particles/mL from $1.92x10^{12}$ to $4.79x10^{12}$, approximately 2.5-fold increased when the hydrophilic photosensitizer was incorporated.

(A)

Formulations	Particle Size (nm)	PId	Zeta potential	Nanoparticles /mL
unloaded LCN	198.56 (±1.00)	0.281 (±0.02)	-41.13 (±1,10)	1.92×10^{12}
AlClPc-loaded LCN	179.7 (±2.05)	0.131 (±0.02)	-44.23 (±0,75)	4.79×10^{12}

(B)

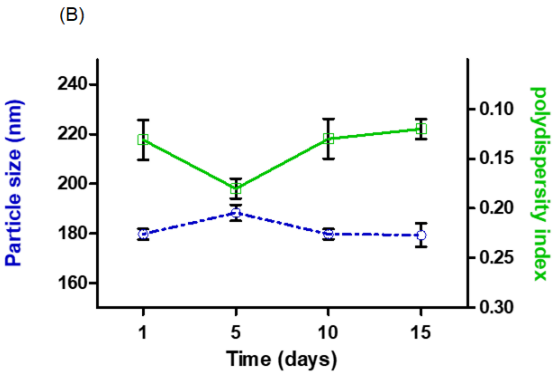

Figure 3. Results of mean particle diameters (Particle Size), polydispersity index (PDI), zeta potential and Nanoparticle Tracking Analysis (Nanoparticles/mL), and Physical stability evaluations during 15 days post preparation.

The next task was evaluated the colloidal stability of the LCN containing AlClPc during 15 days at room temperature, with respect to the mean diameter and polydispersity index (Pld) by DLS. As expected, there were no differences in average of particle size or even polydispersity index during experimental period (**Figure 3. B**). We attribute these results to the presence of poloxamer into the system. In fact, the colloidal stability

of LCN have been achieved with concentrations of poloxamer above 0.4 (w/w) in relation to the aqueous phase (Landh 1994). Poloxamer 407, also known as Pluronic F-127 or Synperonic PE/F 127, is a non-ionic surfactante containing hydrophilic character. It is a copolymer composed by polypropylene glycol and polyethylene glycol (Gilles et al., 2006). This stabilizing effect produced by poloxamer 407, can occur due to insertion of the propylene oxide units in the lipid bilayer of the system, while the polyethylene oxide units solubilize in the aqueous region [Silvestrini et al., 2020). Herein, we choose to use poloxamer amounts higher than 0.4, such as 1.5 in relation to aqueous phase (w/w), to guarantee the steric stability provided by poloxamer 407. Together these physicochemical aspects of the LCNs were similar to that described in the literature for different LCNs systems (Silvestrini et al., 2020; Zhai et al., 2019; Manaia et al., 2017).

The figure 4 sumarize the biocompatibility of unloaded LCN and AlClPc -LCN using normal skin cells (HaCat) and tumor skin cells (A375) in the dark. The samples tested did not show significant cytotoxicity, with most cell viability rates above 80% except for the samples contanining AlClPc concentration above 600 ng/mL (**Figure 4. A**).

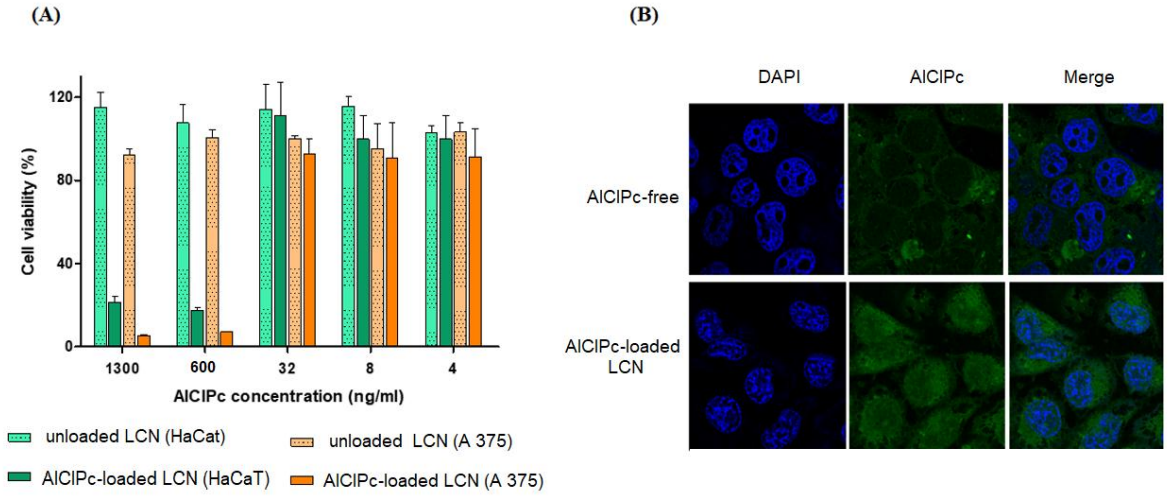

Figure 4: In vitro biocompatibility test of LCN unloaded and AlClPc-loaded LCN in the range of 1300 to 4 ng/mL (in the dark) using normal keratinocytes cell-HaCaT and melanoma cell-A375 (A), and intracellular internalization of AlClPc -loaded LCN at 30 ng/mL using melanoma cell (B).

Considering this result, we can conclude that cell viability was affected by AlClPc in the dark in a dose dependente manner. Because of this, the next experiments were carried out using AlClPc-loaded LCN concentration less than 600nm, since potential photosensitizers must have low dark cytotoxicity and strong phototoxicity. Furthermore, all cell lines treated with unloaded LCN showed high viability at the same highest photosensitizer concentration, demonstrating that nanoparticles does not affect cell viability in the absence of AlClPc. Our next goal was to confirm the ability of LCN to promote AlClPc cellular uptake by confocal microscopy, and as a result, the AlClPc was efficiently internalized by cells displaying cytoplasmic localization. In the merged images, it is possible to visualize a strong AlClPc green fluorescence around the DAPI stained nucleus (blue fluorescence) evidencing the cell-wide distribution of AlClPc-loaded LCN in the cytoplasm of melanoma cells (Figure 4. B). Due to the natural fluorescent properties of AlClPc this also opens a possibility for future use of this AlClPc-loaded LCN as a theranostic plataform.

On the other hand, the AlClPc free showed a weak fluorescence suggesting a lower transfection rate by itself and its consequent degradation when compared to nanoparticles. It is important to say that AlClPc is insoluble in water, which has limited cell penetration. Also, in aqueous medium this molecule may undergo aggregation in which, directly affects its photophysical properties (Calori et al., 2016). To overcome this advantage we rightly chose to load AlClPc through lipid systems as LCN which can be readily internalized through the cells by endocytosis due to lipids componentes of cell membranes and the similar lipids components of the nanoparticle (Ana Review). Herein the LCN were prepared by mixture of aqueous and lipid phase containing monoolein (MO) and oleic acid (OA) which have proven permeation enhancer properties due their similarity with cellular membrane structure (Campos et al., 2020; Rossetti et al., 2016; Praça et al., 2012; Rossetti et al.,2011; Lopes et al., 2006).

MO is an unsaturated monoglyceride containing character amphiphilic, biodegradable, biocompatible and non-toxic, making it a potent lipid to encapsulate both hydrophobic and hydrophilic molecules (Kulkarni et al., 2011). It is able to alter the cell membrane barrier properties due to interactions with the cellular lipids in the cell membrane and to modulate PS delivery (Lopes et

al., 2007). In addition to MO, the OA also influences the cell membrane lipids, favoring the delivery of drugs to the cytoplasm. Furthermore, the nanometric size of the hexagonal liquid crystalline particles used in this work such as lower than 200nm, facilitated cell transfection of AlClPc-loaded LCN in A 375 cell line. (Borgheti-Cardoso et al., 2020). Previously, we reported that the use of LCN based on monoolein and oleic acid as dermal delivery system of different photosensitizers (chlorine and zinc phthalocyanine), also provide additional advantages as protection for degradation, controlled skin delivery, increased stability of photosensitizer and therapeutic effect with reduced photosensitizer amounts (Rossetti et al., 2016. Petrilli et al.,2016; Praça et al., 2012).

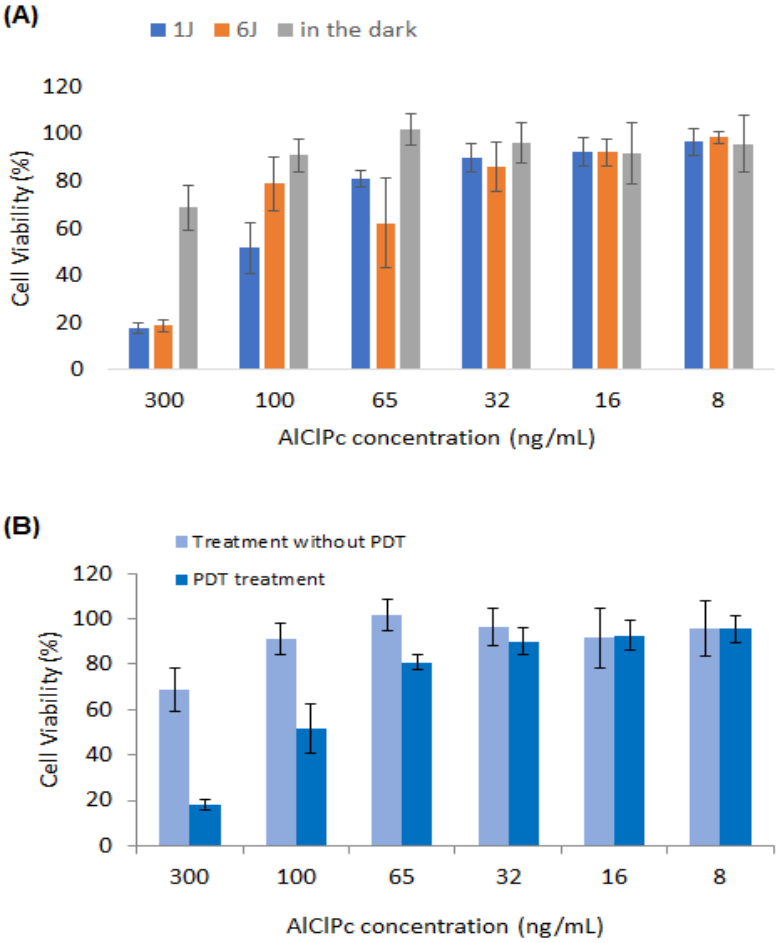

Figure 5: Two different irradiation doses were performed after 24h of A375 incubation with AlClPc -loaded LCN in the range of 8 to 300 ng/mL to select the PDT irradiation protocol such was 1 and 6 J/cm^2 (A) and PDT treatment at J/cm^2 using AlClPc -loaded LCN at final concentration in the range of 8 to 300 ng/mL (B).

In this work, PDT efficiency was directly related to the energy density applied to the A375 cells (1 or 6 J/cm^2) and AlClPc-loaded LCN concentration during 24 hours of treatment. (**Figure 5. A**). At the lowest light dose applied (1 J/cm^2), cell viabilities after treatment with AlClPc-loaded LCN (100ng/mL) was 1.76-fold decreased (from 90.9% to 51.61%) compared to untreated cells. When compared to 6 J/cm^2 applied light dose, the cell viability was 1.53-fold decreased (from 79% to 51.61). There was no significant difference between the light doses applied when AlClPc-loaded LCN at 300ng/mL was used, suggesting that at determined concentrations of AlClPc carried by LCN, the applied dose required to decrease cell viability may be reduced. Therefore, the following experiments were performed only using 1 J/cm^2 as applied light dose for treatment.

Thus, therapy efficacy was confirmed when AlClPc-loaded LCN at 100 and 300 ng/mL was used for 24 hours in A 375 cells (**Figure 5. B**). Cells treated with AlClPc-loaded LCN at 100 ng/mL and irradiation showed a significant decrease (p 0.05) in the cellular viability compared to cells treated without PDT (in the dark), which was 1.76-fold decreased. When the photosensitizer concentration was increased to 300ng/mL, the cell viability decreased was pronounced to 3.84-fold decreased.

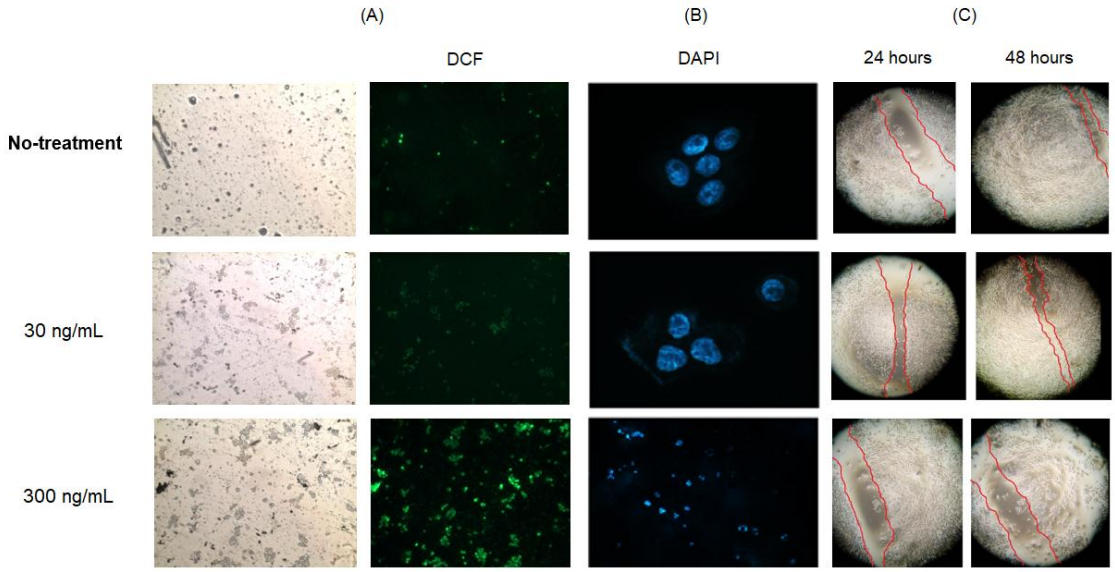

Figure 6: Evaluations of Reactive Oxigen Species Generation (A), Nucleus Damage (B) and Cells Migration (C) followed PDT treatment with AlClPc -loaded LCN at 30 and 300 ng/mL. Untreated cell was used as control.

In PDT, photosensitizers absorb visible light and convert energy to surrounding molecular oxygen and generate a range of highly ROS (Zhou et al., 2016), which cause severe cellular damage including DNA damage (Zhia et al., 2020). To investigate whether A 375 cells affected by PDT with AlClPc-loaded LCN promoted the generation of ROS, the present study detected intracellular ROS generation using DCFH-DA reagent. Considering the fluorescence intensity of DCF detected by fluorescent microscopy such DCF-stained appeared green, the results demonstrated a strong intracellular green fluorescence when A 375 cells were treated with AlClPc-loaded LCN at 300 ng/mL and irradiation **(Figure 6. A).** To the other tested protocols (untreated cells and PDT with AlClPc-loaded LCN at 30 ng/mL used as control sample and LCN containing AlClPc at non-phototoxicity concentration for A 375, respectively), this intracellular green fluorescence was less pronounced.

In addition to labeling of cells with DCF, we provided a qualitative analyse about nucleus damage by fluorescence microscopy. In this assay, the DAPI-stained nuclei appeared blue. Results showed a decrease in the blue fluorescence intensity along with reduced size of the nucleus for tested PDT using AlClPc-loaded LCN at 300ng/mL (**Figure 6. B**), suggesting that PDT evaluated in this work promoted cell death through apoptosis procedure.

Apoptosis have been considered to be the dominant type of cell death in the PDT procedure. Previously, Dmitrieva and Burg (2008), described that apoptotic cells can be identified by the chromatin condensation that occurs during apoptosis. The intensity of DAPI staining increases when the chromatin in nuclei is condensed, raising maximal DAPI pixel intensity. Also, chromatin condensation reduces the nucleus size and consequently a nuclear area reduction (Dmitrieva et al., 2008). Thus, the present study observed typical apoptotic cells with nuclear fragmentation following PDT and AlClPc-loaded LCN as delivery system. This effect was probably due to the increased level of ROS.

To further examine the effect of A 375 cell migration capacity after PDT, the scratch wound healing assay was employed. Following 24 and 48 hours of incubation, cells treated with PDT using AlClPc-loaded LCN at 30 ng/mL, exhibited a similar migration distance to those treated without PDT (in the dark). However, cells treated with PDT using AlClPc-loaded LCN at 300 ng/mL (10 times higher photosensitizer concentration), notably decreased migration into the wound in a AlClPc dose dependent manner (**Figure 6. C**). This result indicated that AlClPc-loaded LCN and PDT may be a powerful tool in the inhibition of cell metastasis.

4. CONCLUSION

The present study assessed the PDT effects of AlClPc-loaded LCN on cancer cells. Based on obtained results, it was confirmed that LCN as delivery system-based nanotechnology to AlClPc in PDT was stable, particles size less than 200nm, exhibited adequate cell transfection, inhibited cell migration, induced phototoxicity and melanoma cell apoptosis by producing ROS. We believe that LCN containing AlClPc is a promising delivery system for the photodynamic treatment. Further additional studies will be valuable to confirm its clinical application.

Declaration of competing interest

The authors declare that there are no conflicts of interest in this work.

ACKNOWLEDGEMENTS

This work was developed within the framework of National Institute of Science and Technology of Pharmaceutical Nanotechnology (INCT-Nanofarma), which is supported by São Paulo Research Foundation (FAPESP, Brazil, grant #2018/08253-9) and National Council for Scientific and Technological Development (CNPq, Brazil, grant #465687/2014-8).

REFERENCE

1. Borgheti-Cardoso, Livia Neves; Viegas, Juliana Santos Rosa; Silvestrini, Ana Vitoria Pupo; Caron, Angelo Luis; Praça, Fabiola Garcia; Kravicz, Marcelo; Bentley, Maria Vitoria Lopes Badra (2020). Nanotechnology approaches in the current therapy of skin cancer. Advanced Drug Delivery Reviews, (), S0169409X20300119, 2020.
2. Calori IR, Tedesco AC. Lipid vesicles loading aluminum phthalocyanine chloride: formulation properties and disaggregation upon intracellular delivery. Journal of Photochemistry and Photobiology B: Biology., 2016; 160: 240-7.
3. Campos, P.M., Praça, F.G., Mussi, S.V. et al. Liquid crystalline nanodispersion functionalized with cell-penetrating peptides improves skin penetration and anti-inflammatory effect of lipoic acid after in vivo skin exposure to UVB radiation. Drug Deliv. and Transl. Res., 2020; 10: 1810–1828.
4. Dmitrieva Natalia I.; Maurice B. Burg. Analysis of DNA breaks, DNA damage response, and apoptosis produced by high NaCl. Am J Physiol Renal Physiol, 2008; 295(6): 1678–1688.
5. Ferreira, Hadma Sousa, & Rangel, Maria do Carmo. Nanotecnologia: aspectos gerais e potencial de aplicação em catálise. Química Nova, 2009; 32(7): 1860-1870.
6. Fong C, Le T, Drummond CJ. Lyotropic liquid crystal engineering–ordered nanostructured small molecule amphiphileself-assembly materials by design. Chem. Soc. Rev., 2012; 41: 1297–1322.
7. Gilles Dumortier; Jean Louis Grossiord; Florence Agnely; Jean Claude Chaumeil. A Review of Poloxamer 407 Pharmaceutical and Pharmacological Characteristics, 2006; 23(12): 2709–2728.
8. Huang Y, Gui S. Factors affecting the structure of lyotropic liquid crystals and the correlation between structure and drug diffusion. RSC Adv., 2018; 8: 6978–6987.
9. Koechli, O. R., Schaer, G. N., Schenk, V., Haller, U., & Walt, H. Assessment of effect of photosensitizers on cytotoxicity of photodynamic therapy in human breast cancer cell cultures. Archives of gynecology and obstetrics, 1995; 256(4): 167–176.
10. Krattinger R., M.J. Barysch, E. Ramelyte, S. Micaletto, S.M. Goldinger, F. Dimitriou, R. Dummer, The World of Melanoma: Epidemiologic, Genetic, and Anatomic Differences of Melanoma Across the Globe, Curr. Oncol. Rep., 2018; 20.
11. Kulkarni C V., Wachter W, Iglesias-Salto G, et al. Monoolein: A magic lipid? Phys. Chem. Chem. Phys., 2011; 13: 3004–3021.
12. Landh T. Phase Behavior in the System Pine Needle Oil Monoglycerides-Poloxamer 407-Water at 20.degree. J. Phys. Chem., 1994; 98: 8453–8467.
13. Lopes LB, Lopes JLC, Oliveira DCR, Thomazine JA, FantiniMCA, Collett JH, et al. Liquid crystalline phases of monooleinand water for topical delivery of cyclosporin A: characterization and study of in vitro and in vivo delivery. Eur J Pharm Biopharm., 2006; 63: 146–55.
14. Lopes Luciana B.; Fernanda F.F. Speretta; M. Vitória L.B. Bentley (2007). Enhancement of skin penetration of vitamin K using monoolein-based liquid crystalline systems., 2007; 32(3): 209–215.
15. Manaia EB, Abuçafy MP, Chiari-Andréo BG, et al. Physicochemical characterization of drug nanocarriers. Int. J. Nanomedicine., 2017; 12: 4991–5011.
16. Medina, W. S. G. ; Praça, Fabíola Silva Garcia ; Aline Carollo ; Bentley, Maria Vitória Lopes Badra . Nanocarriers to deliver photosensitizers in topical photodynamic therapy and photodiagnostics. In: Beck, Ruy; Guterres, Silvia; Pohlmann, Adriana. (Org.). New Approaches for Skin Care. 1ed.: Springer Publishing, 2011; 1: 287-310.
17. Petrilli R., J.O. Eloy, F.S.G. Praça, J.O. Del Ciampo, M.A.C. Fantini, M.J.V. Fonseca, M.V.L.B. Bentley, Liquid crystalline nanodispersions functionalized with cell-penetrating peptides for topical delivery of short-interfering RNAs: A proposal for silencing a pro-inflammatory cytokine in cutaneous diseases, J. Biomed. Nanotechnol., 2016; 12: 1063–1075.
18. Praça Fabíola Garcia, Juliana Santos Rosa Viegas, Hong Yong Peh, Tuane Nardacchione Garbin, Wanessa Silva Garcia Medina, Maria Vitoria Lopes Badra Bentley, Microemulsion co-delivering vitamin A and vitamin E as a new platform for topical treatment of acute skin inflammation, Materials Science and Engineering: C, 2020; 110: 110639.
19. Praça FSG, Medina WSG, Petrilli R, Bentley MVLB. Liquid crystal nanodispersions enable the cutaneous delivery of photosensitizerfor topical PDT: fluorescence microscopy study of skin penetration.Curr Nanosci., 2012; 8: 535–40.
20. Rossetti F C ; Depieri L V; Praça, FS; CIAMPO, J. O.; FANTINI, M. C. A.; Maria Bernadete Riemma Pierre; TEDESCO, Antonio Claudio; BENTLEY, MARIA VITÓRIA L.B. . Optimization of protoporphyrin IX skin delivery for topical photodynamic therapy: Nanodispersions of liquid-crystalline phase as nanocarriers. European Journal of Pharmaceutical Sciences, 2016; 83: 99-108.
21. Rossetti FC, Fantini MCA, Carollo ARH, Tedesco AC, BentleyMVLB. Analysis of liquid crystalline nanoparticles by small angleX-ray diffraction: evaluation of drug and pharmaceutical

additivesinfluence on the internal structure. J Pharm Sci., 2011; 100: 2849–57.
22. Silvestrini, Ana vitoria Pupo; Caron, Angelo Luis; Viegas, Juliana; Praça, Fabíola Garcia; Bentley, Maria Vitoria Lopes Badra . Advances in lyotropic liquid crystal systems for skin drug delivery. Expert Opinion on Drug Delivery, 2020; 1: 1-25.
23. Zhai J, Fong C, Tran N, et al. Non-Lamellar Lyotropic Liquid Crystalline Lipid Nanoparticles for the Next Generation of Nanomedicine. ACS Nano., 2019; 13: 6178–6206.
24. Zhia Defu, Ting Yang, Justin O'Hagan, Shubiao Zhang, Ryan F. Donnelly. Photothermal therapy. Journal of Controlled Release, 2020; 325: 52–71.
25. Zhou Zijian, Jibin Song, Liming Nie, Xiaoyuan Chen. Reactive oxygen species generating systems meeting challenges of photodynamic cancer therapy. Chem Soc Rev., 21, 2016; 45(23): 6597-6626.